Title

Clutch size, but not growth rate, differs between genetically well-mixed populations of the mysid *Neomysis americana* (S.I. Smith, 1873) in Chesapeake Bay tributaries with differing water quality

Authors

Ryan J. Woodland [a,*], Danielle M. Quill [a], Louis Plough [b], Joseph T. Molina [a], Theresa Murphy [a], Oliver Autrey [a,], and Gesche Winkler [c]

Affiliations

[a] Chesapeake Biological Laboratory, University of Maryland Center for Environmental Science, Solomons, MD 20688, USA;

Email addresses: R. Woodland *woodland@umces.edu* (*corresponding author); D. Quill *dquill@umces.edu*, J. Molina *joseph.t.molina@gmail.com*; T. Murphy *tmurphy@umces.edu*; O. Autrey *ollieautrey@gmail.com*

[b] Horn Point Laboratory, University of Maryland Center for Environmental Science, Cambridge, MD 21613, USA;

Email address: L. Plough *lplough@umces.edu*

[c] Institut des sciences de la mer, Université du Québec à Rimouski, Québec-Océan Rimouski, Québec, G5L 3A1, CAN;

Email address: G. Winkler *gesche_winkler@uqar.ca*

Abstract

Small crustaceans such as the mysid *Neomysis americana* (S.I. Smith 1873), are a central component of coastal food webs and, while generally tolerant of a wide-range of environmental conditions, can be negatively affected by poor water quality. In this study, daily growth rates (GR_D) and clutch size metrics of *N. americana* collected during the early and late summer of 2018–2019 were evaluated for the Choptank and Patuxent rivers, major tributaries of Chesapeake Bay known to exhibit different oxygenation regimes. Genetic variation in the mitochondrial CO1 locus was assessed to evaluate the potential intraspecific genetic structure within Chesapeake Bay. CO1 haplotype network analysis, phylogenetic analysis, and AMOVA revealed no genetic differences between Choptank and Patuxent river populations, with all Chesapeake Bay individuals belonging to a single genetic lineage (Lineage C), of the *N. americana* cryptic species complex. Total and size-specific clutch size were approximately 18% and 53% higher, respectively, in the normoxic Choptank River during the early summer. Embryos within the marsupium, corrected for clutch size and female length, were consistently larger in the Choptank River during later larval development stages. Size-specific clutch size showed correlations with bottom water dissolved oxygen concentration (positive) and water temperature (negative). GR_D did not differ between rivers or seasonally but juveniles grew twice as fast as adults. Given that all individuals genotyped from both rivers belonged to lineage C of the *N. americana* cryptic species complex, it is hypothesized that bottom water hypoxia (rather than genetic differentiation) is responsible for reduced clutch size in the Patuxent River. Our findings build on other recent work by providing evidence of a direct, negative relationship between hypoxia and local population dynamics of *N. americana*, a key ecological component of Chesapeake Bay's food web.

Key words: connectivity, invertebrate, water quality, population, modal length analysis

Statements and Declarations

This work was supported by Maryland Sea Grant award #07-5-25839, National Science Foundation award OCE-2023349 (UMCES) and OCE-1756244 (Maryland Sea Grant REU Program), and Chesapeake Biological Laboratory. RJW, OA, and LP contributed to the study conception and design. Material preparation, data collection, and analysis were performed by all authors. The first draft of the manuscript was written by OA and RJW and all authors commented on previous versions of the manuscript. IACUC permissions were not required as part of this research. All authors read and approved the final manuscript. The authors have no relevant financial or non-financial interests to disclose.

1. Introduction

Coastal ecosystems are among the most productive areas on Earth, providing ecosystem services valued at billions of dollars annually (Liquete et al. 2013). Much of the socioeconomic value of coastal ecosystems arises from their ecological productivity, yet human development in coastal areas and upstream watersheds has degraded many coastal ecosystems (Lotze et al. 2006). Common symptoms of this degradation, including habitat loss, hydrodynamic changes, sedimentation, and eutrophication, can impair the functioning of coastal systems by altering the identity and relative productivity of different food web components. Further, differences in local environmental conditions within ecosystems, whether natural or human-induced, can lead to spatially explicit patterns in ecosystem productivity (Kennish 2002; Cottenie 2005; Elliott and Whitfield 2011). Understanding the bottom-up effects of local environmental conditions (human-mediated and natural) on coastal food web productivity is an area of intense research interest given its potential to influence nearly every facet of ecosystem dynamics, from water chemistry and biogeochemical cycling to biotic community structure (Nyström et al. 2012).

In many coastal systems, planktonic food webs represent a dominant source of primary and secondary production supporting higher trophic levels. Mysids, small shrimp-like crustaceans that are globally distributed in aquatic ecosystems, occupy pivotal positions in many coastal pelagic food webs. Mysid concentrations can exceed 10^5 individuals m^{-3} (Jumars 2007) with different species capable of inhabiting either (or both) shallow and deeper water areas. Mysids are highly mobile, often displaying pronounced inshore-offshore or vertical movements over (sub)daily, seasonal, or annual cycles (Jumars 2007). As consumers, mysids are capable of feeding on a broad range of plants, animals, and organic matter that can include phytoplankton, microphytobenthos, zooplankton, zoobenthos, detritus, and other small taxa (Mauchline 1980;

Zagursky and Feller 1985; e.g., Froneman 2001; Winkler et al. 2003). In turn, mysids are consumed by a wide array of invertebrate and vertebrate predators, sometimes representing the dominant prey taxon (by biomass) consumed by small-bodied adult or juvenile life-stage fishes in coastal areas such as Chesapeake Bay, USA (Hines et al. 1990; Buchheister and Latour 2015; Ihde et al. 2015; Pagenkopp Lohan et al. 2023). Because of their abundance, high mobility, omnivorous diet, and importance as prey, mysids are important integrators of environmental and basal trophic conditions that support higher trophic levels in coastal ecosystems.

Despite the central role of mysids in many coastal food webs, knowledge of environmental controls on vital rates and population dynamics of many species is incomplete or entirely absent in some instances. For example, mysid growth and reproduction (clutch size and progeny size) have been linked to food availability, salinity, and water temperature but the relative importance of these different factors appears species- and location-specific (Winkler and Greve 2002; Fockedey et al. 2005; Paul and Closs 2014; Akiyama et al. 2015). Positive food-clutch size relationships have primarily been observed in oligo-mesotrophic systems or shallow eutrophic systems where the potential for negative ecological effects of increased primary production are minimal (e.g., Bouchard and Winkler 2018). It is unclear whether the positive effect of high local productivity on mysid reproductive output might be offset by the formation of hypoxia and the attendant possibility of negative physiological and ecological effects on mysids in more eutrophic ecosystems. This knowledge gap is particularly important given the potential effects of nutrient reduction efforts (as a means of curtailing hypoxia; Breitburg et al. 2018) on the ecological footprint of mysids in coastal systems.

In this study, we conducted a natural experiment by assessing genetic connectivity and comparing growth rates and clutch size metrics between populations of the mysid *Neomysis*

americana (SI Smith 1873) between two tributaries of Chesapeake Bay, the Patuxent and Choptank rivers. Given the unknown population connectivity of *N. americana* across Chesapeake Bay tributaries, we analyzed the genetic structure of mysids from the Patuxent and Choptank rivers as a first step toward evaluating the extent to which genetic differentiation, in conjunction with environmental exposure, differed between the two populations. These tributaries have very similar temperature and salinity regimes but differ in their basin morphology, nutrient regimes, chl-α concentrations, and prevalence of seasonal hypoxia (Kemp et al. 2005; Fisher et al. 2006). Quillen et al. (2022) recently documented lower trophic position and increased reliance on pelagic trophic pathways among *N. americana* in the Patuxent River compared to the Choptank River, suggesting bottom water quality differences between the two tributaries may be driving bottom-up changes in diet. Further, Patuxent River mysids had a lower whole-body carbon:nitrogen tissue ratio, a proxy marker of lipid and protein content and potential indicator of physiological condition (e.g., Donnelly et al. 1993; Lehtiniemi et al. 2002). We hypothesized that these trophic and condition differences between the two rivers would lead to reduced growth rate and reduced clutch size within the Patuxent River population of *N. americana* relative to the Choptank River population.

2. Materials & Methods

2.1 Study area

The focal study area included the oligo- to mesohaline reaches of the Patuxent and Choptank rivers, two tributaries of Chesapeake Bay located on opposing shores of the Bay (Figure 1). Their similar latitude and distance from the Bay mouth results in comparable salinity and temperature regimes between the tributaries (Fisher et al. 2006). For example, daily average

surface salinities and water temperatures at the mouth of each tributary recently ranged 6–16 and 2–30 °C, respectively, in the Patuxent River, and 3–14 and 1–30 °C, respectively, in the Choptank River, depending on river discharge, winds, and tidal conditions (Patuxent River NOAA monitoring Station SLIM2 – 8577330, www.ndbc.noaa.gov; Choptank River CBP monitoring station E5.2, https://eyesonthebay.dnr.maryland.gov; 2018–2022 data, *accessed* 02/15/2024). Despite these similarities, differences in basin bathymetry and geomorphology result in seasonally recurrent hypoxia (dissolved oxygen concentration < 2 mg/L) in the bottom waters of the mid-to-lower reaches of the Patuxent River that is generally absent in the Choptank River (Fisher et al. 2006; Quillen et al. 2022). To evaluate differences in bottom water quality at oligo- and mesohaline areas in each tributary basin, vertical profiles of monthly (January 2018 – December 2019) dissolved oxygen concentration (DO, mg/L), chlorophyll-a concentration (Chl-a, µg/L), salinity (psu scale), and water temperature (WTemp, °C) at 4 long-term monitoring stations were downloaded from the Chesapeake Bay Program Water Quality Monitoring Program's datahub (data.chesapeakebay.net/WaterQuality; Figure 1). The monitoring program collects bottom water measurements within 1–1.5 m of the bottom of the channel at each station. Both rivers have bottom sediments primarily composed of muddy silt and clay in the area of these stations, with sediments ranging 87–93% and 93–95% silt/clay per unit mass for the Choptank and Patuxent rivers, respectively (https://baybenthos.versar.com/data.htm; 2018–2019).

2.1 Study species

Neomysis americana, a regionally abundant mysid and the focal species in this study, is distributed along the northwestern Atlantic coast in oligohaline to euhaline waters and from

surface waters to 250m depth (Tattersall 1951). Like other *Neomysis* spp., *N. americana* are short lived (< 1 year) and sexual maturation is temperature-dependent, resulting in populations supported by multiple recruiting and maturing cohorts each year (Pezzack and Corey 1979; Toda et al. 1983; Fockedey et al. 2005; Viñas et al. 2005). Overwintering *N. americana* females mature slowly and achieve relatively large body sizes prior to spring reproduction; whereas, summer cohorts are composed of rapidly maturing females that reproduce at smaller body sizes (Wigley and Burns 1971; Mayor et al. 2017; Bouchard and Winkler 2018). The number of embryos in the masupium is size-dependent, with egg number increasing as female body size increases and ranging from 5 to ~80 eggs per female (Pezzack and Corey 1979; Mayor et al. 2017; Bouchard and Winkler 2018).

2.2 Field collections

Mysids were primarily collected from the Patuxent and Choptank rivers on night cruises conducted monthly from May through September in 2018 and 2019 (Table 1). Six stations were located in each tributary, with the uppermost station located near the estuarine turbidity maximum in each system and extending downstream at approximately equidistant intervals to the confluence with the mainstem (Figure 1). At each station, a 60-cm diameter zooplankton net (0.8 m^2 sampling area) with 300-µm mesh and attached flowmeter (Sea-Gear ® Corp., Melbourne, FL) was used to collect mysids. The net was towed twice for 3 min perpendicular to the channel, once just below the surface and once at approximately mid-depth. In some instances, the net depth was stepped up or down in the water column during the tow to remain approximately mid-depth. After each tow, the catch was sieved to remove gelatinous

zooplankton and large debris, then stored in individually-labelled jars with 95% buffered ethanol (1:1 sample to preservative ratio).

A small number of *N. americana* were collected in 2018 from two sites on the St. Lawrence Estuary to provide spatial outgroups for the population genetic analysis (Table 1). Mysids were collected at a mid-estuary site (salinity = 15) located in the northern channel of the St. Lawrence Estuary off the Petite Rivière St. François (site name: SL-ES; 47°17.975' N 70°30.888' W, collection date: 29 September), and at an estuarine transition site (salinity = 1.5) located at Saint-Jean-Port-Joli (site name: SL-MTZ; 47°12.95'N; 70°16.39'W, collection date: 19 June).

2.3 Sample sorting

In the lab, preserved samples were subsampled with a Folsom plankton splitter. Subsamples were processed using a dissecting microscope at 1.5–5 × magnification with both reflected and transmitted light. All mysids were sorted, then examined under increased magnification (5–20 ×) to positively identify *N. americana* based on the number and location of spiniform setae on the telson (Heard et al. 2006). Individual *N. americana* were allocated to one of five life-history categories based on length (distance from rostrum to base of the telson), secondary sexual characteristics, and reproductive status (Mayor et al. 2017; Bouchard and Winkler 2018):

- Juveniles < 4 mm length
- Immature > 4 mm and lacking secondary sexual characteristics (marsupium or elongated 4th pleopod)
- Mature male (elongated 4th pleopod)
- Mature female with empty marsupium

- Mature female with full marsupium

2.4 Genetic sample analysis

DNA was extracted from a subset of Chesapeake Bay mysids from the Choptank and Patuxent rivers as well as from mysids collected at two locations on the St. Lawrence Estuary using the E.Z.N.A. tissue DNA kit (Omega Biotek, Norcross GA). Eggs were removed from each extraction individual (if female) to eliminate DNA contamination from offspring. DNA concentration was determined for each extraction using a Qubit 2.0 fluorometer (Invitrogen) with the double-stranded, broad range DNA kit. Once concentrations were recorded, all samples were diluted to ~10 ng/µL in new tubes using Nuclease free water. Once all samples were extracted and diluted, a series of 3 different concentrations (10ng, 30ng, 50ng) of DNA along with a positive (mysid DNA) and negative (no template) control were used to test mitochondrial CO1 gene PCR primers jgLCO1490 and jgHCO2198 primers (Geller et al. 2013), starting with the master mix recommendations of Geller et al. (2013). The following master mix recipe gave the highest amplification success and was then applied to all subsequent samples (volumes per single, 50µl PCR reaction): 10 uL of 5X Gotaq flexi buffer, 4 uL of 25 mg/ml $MgCl_2$, 1uL of dNTPs at 10mM each dNTP, 1.5 uL of F primer jgHCO2198, 1.5 uL of R primer jgLCO1490 (both primers at 10mM), 0.4 uL of Gotaq flexi taq polymerase, 29.6 uL of Nuclease free water, and 3 uL of DNA at ~ 10 ng/µl. The PCR conditions were an initial 5 mins at 95 °C; then 39 cycles of 30s at 95 °C, 45s at 48°C, 1 min at 72°C and a final 5 min at 72°C. Reactions producing no amplification, a weak band, or multiple bands in subsequent agarose gels of the PCR products were repeated until strong, single bands at the target size (~700 bp) were achieved, or the sample was not included for DNA Sanger sequencing. All positive (visible) and correctly

sized PCR products were submitted to the DNAlab at Arizona State University for bi-directional sequencing with the Geller et al. (2013) CO1 primers. The raw Sanger forward and reverse reads for a given sample were denovo assembled in Geneious Prime (2022-2.2) and trimmed to a contiguous region in which the quality scores remained above 20. Sequences were then aligned to each other using Aliview 1.26 (Larsson 2014), trimmed to 594 bp and the alignment was converted to a FASTA file for downstream analyses.

2.5 Mysid processing

Females with full and intact marsupia were set aside for clutch size measurements. Under 1.5–5 × magnification, each female was photographed and its body length (anterior tip of rostrum to base of the telson) measured digitally (Olympus DP73 9 MP digital camera mounted on an Olympus SZX16 stereo dissecting scope, Olympus Cell-Sans 2.1 software). Each marsupium was dissected with fine needles, all contents removed, and embryos were enumerated. For a subsample of these females (n = 61, Table 1), embryos were assigned to one of three developmental stages (Mauchline 1980): Stage 1 (egg), Stage 2 (eyeless pre-larva), and Stage 3 (eyed pre-larva). Embryos were then counted and a subsample (n = 5) measured for diameter (Stage 1) or total length (Stages 2 & 3). Females and Stage 2 and 3 embryos were measured as the sum of 2 or 3 segments of a contiguous line overlaid along the dorsal surface of each individual (Stage 1 embryos were measured as a single straight line through the center of the embryo). Clutch size was measured for females that were collected during May and (or) June (spring-reproducing cohort) and August and (or) September (summer reproducing cohort) in each river during 2018 and 2019 (Table 1).

Modal length analysis was used to calculate growth rates of juvenile and adults. Individual lengths (L) were measured using the ImageJ software (v1.53; Schneider et al. 2012) and digital images collected with the digital camera mounted on the dissecting scope (described above). Mysids were assigned to 0.5-mm incremental length classes and the proportion of measured individuals in each length class was then used to construct the size frequency distribution of mysids collected at each station. The three stations from each tributary that most consistently yielded mysids were selected for growth rate analysis (Patuxent: P2, P3, and P5; Choptank: C3, C4, and C5; Figure 1; Online Resources 1 & 2). Modes within size-frequency distributions from these stations were identified and fitted as a series of overlapping Gaussian curves using the NORMSEP procedure in the FAO-ICLARM Stock Assessment Tool software (FISAT II; Gayanilo et al. 2005). Daily growth rates (GR_D) were determined as the incremental change in location of length modes between months, divided by the number of days elapsed between sampling events. Growth rates were identified as juvenile if the length mode of the earlier month was < 4 mm, otherwise GR_D were identified as adult.

2.6 Data analysis

Genetic data were analyzed to evaluate genetic diversity and population connectivity between mysid populations in the Choptank and Patuxent rivers. Mysid samples from two populations in the St. Lawrence Estuary were also sequenced to provide complementary data from a geographically distant population of *N. americana*. Analysis of mitochondrial CO1 sequences were performed in Mega v 10.1.0 (Kumar et al. 1994) to produce a Neighbor-Joining phylogenetic tree based on the p-distance (Nei and Kumar 2000) method, and was constructed using 999 bootstraps to test the confidence of nodes. All codon positions were utilized and pair-

wise deletions were used for any missing nucleotide. All usable sequences from Chesapeake Bay and St. Lawrence Estuary were included in the tree as well as a CO1 sequence for *Neomysis integer* as an outgroup obtained from Genbank (Genbank Accession #: AJ852595.1). Eighteen previously published *N. americana* sequences from the three observed genetic lineages in Cortial et al. (2019) were also included to allow comparison of the new mysid sequences to the lineages identified previously. The relationships among haplotypes within and between populations was also assessed via the randomized minimum spanning tree approach (RMST; Paradis 2018) and plotted with the '*pegas*' R package v. 1.2 (Paradis 2010). Hierarchical analysis of molecular variance (AMOVA) was implemented in the *pegas* package following Excoffier et al. (1992) to examine partitioning of molecular variance across regions and among populations within regions (in Chesapeake Bay and St. Lawrence Estuary). Haplotype diversity (h) and nucleotide diversity (π) were calculated for each population separately and in a combined, within-region population set (Chesapeake Bay vs St. Lawrence Estuary) in *pegas*. Finally, pairwise Phi-st estimates were calculated in *pegas* and confirmed with the 'pair-Phist' function in the '*haplotype*s' R package (Atkas 2023).

An exponential regression fitted to clutch size vs female body length (L_f) using least-squares means was fitted to the data but only explained 30% of the variability in the data ($F_t = 2.554e^{0.254 \cdot L_f}$, $R^2 = 0.30$; *not shown*). To further explore the relationship between clutch size, L_f, and potential spatiotemporal predictors, a generalized linear model (GLM) with Poisson distribution (log link) was fitted. Predictor variables in the clutch size model included two categorical variables (tributary: Patuxent, Choptank; Season: Early summer [May, June], Late summer [August, September]), L_f as a continuous variable, and all possible interactions.

283 Size-specific clutch size (C_{ss} [embryos / mm] = number of embryos / female body length)
284 and growth rates were analyzed using GLMs with a Gaussian distribution and either a log (C_{ss}
285 model) or an identity (growth model) link. Predictor variables in the C_{ss} model included
286 tributary, season, L_f, and all possible interactions. Predictor variables included in the growth
287 model included tributary, season, life stage (juvenile, adult), and all possible interactions. Year
288 was not included as a factor in any of the models due to the unbalanced nature of the dataset
289 between years (Table 1). All GLMs were fitted using iteratively reweighted least squares with
290 the *glm*() function using RStudio (v2023.12.0) with the R Statistical Software (v4.3.1; R Core
291 Team 2023). Variable significance was determined by *F*-tests with degrees of freedom estimated
292 using Satterthwaite approximation.

293 Embryo size as a function of clutch size and female body length (L_f) was compared
294 between tributaries to assess growth of embryos prior to release from the marsupium. Using the
295 subset of gravid females for which embryo size data were available, mean embryo size was
296 divided by clutch size (E_l:C_t = mm / embryo). This ratio was then regressed against L_f separately
297 for each embryo stage. To account for the curvilinear relationship between E_l:C_t and L_f, negative
298 exponential models ($E_l: C_t = \alpha e^{-\beta \cdot L_f}$) were fitted using least-squares regression. Tributaries
299 were compared by analyzing residuals from each model using two-way ANOVA (categorical
300 factors: Tributary, Embryo stage).

301 Growth rates were analyzed using multifactor ANOVA with tributary, season, and life
302 stage (Juvenile, Adult) as predictors, along with all possible interactions. Preliminary testing
303 indicated that no interactions were present (interaction term *F*-tests, $F \geq 2.72$, $p \geq 0.11$),
304 therefore, the final model included only main effects. Parametric assumptions of the ANOVA,
305 GLM, and regression models for clutch and growth models were evaluated using visual

assessment of residual plots and statistical tests for normality and homogeneity of variance. All tests were deemed satisfied.

Kendal rank correlation analysis was used to evaluate relationships between clutch size, C_{ss} and bottom water quality variables. Clutch size metrics were averaged for every combination of station, river, month and year, then analyzed for correlations with monthly water quality values at either the oligohaline or mesohaline reach of the estuary based on proximity of CBP stations to local water quality monitoring sites (Figure 1). Bottom water quality variables, including DO, Chl-a, salinity, and WTemp, from the same stations and data source used to assess local water quality conditions (described above).

3. Results

3.1 Water quality

Bottom water salinity and temperature showed similar seasonal trends in both tributaries but there were differences in seasonal dissolved oxygen and chlorophyll concentrations (Figure 2). During the May–September sampling period, mean salinities at the oligo- and mesohaline monitoring sites in each tributary were 0.4 ± 0.7 (SD) and 8.3 ± 2.0 in the Choptank River and 0.6 ± 1.5 and 9.7 ± 2.2 in the Patuxent River. Bottom water temperatures were much more similar between monitoring sites within tributaries, with mean May–September water temperatures of 25.6 ± 3.7 °C and 25.1 ± 3.5 °C (oligohaline and mesohaline, respectively) in the Choptank River and 25.0 ± 4.8 °C and 23.8 ± 4.3 °C in the Patuxent River. Chlorophyll concentrations were approximately two times greater at the oligohaline Patuxent site (29.2 ± 8.9 µg/L) than the Choptank River site (16.6 ± 8.1 µg/L) from May–September, but were much more similar at the downstream mesohaline sites (Patuxent = 5.3 ± 5.8 µg/L; Choptank = 7.7 ± 4.2

329 µg/L). Bottom water dissolved oxygen concentration showed an opposite pattern during the
330 May–September interval, with similar concentrations present at oligohaline sites on both rivers
331 (Choptank = 5.7 ± 8.1 mg/L, Patuxent = 6.6 ± 1.5 mg/L) but a higher average concentration at
332 the mesohaline Choptank site (4.9 ± 0.9 mg/L) than the mesohaline Patuxent site (2.9 ± 2.5
333 mg/L).
334
335 *3.2 Genetic diversity of N. americana*
336 A total of 51 high-quality sequences 594 bp in length were generated across the four collection
337 sites: 17 from the St. Lawrence Estuary (STL) populations, 35 from the Chesapeake Bay
338 populations. A total of 38 unique haplotypes were identified among all samples, with 65 variable
339 nucleotide positions across 594 bp. Haplotype diversity (h) and nucleotide diversity (π) varied
340 among populations, with greater diversity generally found in the Chesapeake Bay populations
341 (Table 2). When combining data from populations within a region, h was ~0.97 ± 0.0004 in
342 Chesapeake Bay vs. ~0.91 ± 0.003 (variance) in the St. Lawrence Estuary. Nucleotide diversity
343 appeared to be almost 2-fold higher in STL populations (0.01 vs 0.006, ± 0.00001), but the
344 presence of two, highly-divergent haplotypes was driving this result. When those two sequences
345 were removed (STL-ES-8, STL-MTZ-5), estimates of π in the combined St. Lawrence
346 populations were actually lower than the Chesapeake Bay (~0.003 in STL vs .006 in Chesapeake
347 Bay; Table 2), though sample sizes were roughly ½ that of Chesapeake Bay. Additional analyses
348 suggest that these two haplotypes represent a 3rd divergent lineage of *N. americana,* distinct from
349 the Chesapeake Bay lineage and the other St. Lawrence Estuary lineage (see below). Pairwise
350 divergence estimates in p-distance (percent difference) of sequences within and between
351 populations, and the within-STL p-distance estimates appear to be bi-modal with the two

352 divergent haplotypes producing pairwise divergence estimates of 4–5% compared with the
353 remaining comparisons at or below 1% (Online Resource 3). Within-region pairwise sequence
354 divergence estimates for the Chesapeake Bay populations were consistently between 0 and 2%,
355 likely representing typical intraspecific diversity, while across regions (STL vs Chesapeake)
356 pairwise divergence was between 4–6%. Note that comparisons of *N. americana* sequences with
357 the congener outgroup *Neomysis integer* produced divergence estimates between 9 and 10%.
358
359 *3.3 Genetic structure and partitioning of diversity among populations of N. americana*
360 The Neighbor-Joining tree including all *N. americana* samples, previously published *N.*
361 *americana* sequences from Cortial et al. (2019), and *N. integer* as an outgroup showed clear
362 regional genetic structure, with high bootstrap support (>95%) for three clades, two of which
363 contained sequences from only the St. Lawrence Estuary, and the other containing sequences
364 from the Chesapeake Bay (Figure 3). All Chesapeake Bay samples were found interchangeably
365 among nodes of the tree within the "Chesapeake" clade or lineage (Lineage C from Cortial et al.
366 2019) while all St. Lawrence Estuary samples were found within one of the two St. Lawrence
367 clades or lineages (Lineage A or B). The two divergent haplotypes (ES-8 and MTZ-5) from the
368 St. Lawrence Estuary samples were found in the clade containing sequences from Lineage B in
369 Cortial et al (2019), confirming the presence of this divergent lineage observed in previous
370 studies. A randomized minimum spanning tree (RMST) haplotype network was generated and
371 showed similar trends in spatial patterns of haplotype diversity (Figure 4). The St. Lawrence
372 Estuary samples had no overlapping haplotypes with any of the Chesapeake Bay populations, but
373 within each region, some haplotypes were shared among populations. The two divergent
374 haplotypes from the St. Lawrence Estuary appear as a very distinct cluster in the STL side of the

network, with 21 mutations separating those haplotypes from the other St. Lawrence cluster. Finally, a hierarchical analysis of molecular variance (AMOVA) confirmed substantial variation in haplotypes across regions, with evidence of an effect of region ($p < 0.0001$, region in global: Phi-CT = 0.936) but not of population within region ($p = 0.92$, Phi-SC = -0.0734, i.e., little variation among haplotypes from the Choptank River vs. Patuxent River in the Chesapeake Bay or STL-ES vs STL-MTZ populations in the St. Lawrence Estuary). A similar result was obtained using the PairPhist function in the '*haplotypes*' package to estimate pairwise PhiSt. Pairwise PhiSt analyses between the St. Lawrence Estuary (STL-ES and STL-MTZ populations combined), the Choptank River, and Patuxent River populations showed high heterogeneity between STL and the two Chesapeake Bay populations (PhiST ~ 0.81–0.82, $p < 0.0001$) while PhiSt between the two populations in Chesapeake Bay was essentially zero (PhiST~ -0.008, $p = 0.76$).

3.3 Clutch size

Clutch-size data were available for 307 females with intact and undamaged marsupia (Table 1). Gravid females were smaller (2-way ANOVA, predictor: Tributary, F-statistic $_{df\,(\text{num., den.}) = 2,\,304} = 12.17$, $p < 0.0001$) in the Choptank than the Patuxent with L_f values of 6.97 ± 0.11 mm (least-squares means estimate [LSM] ± SE) and 7.51 ± 0.11 mm, respectively (Figure 5). Seasonally, gravid females were larger (2-way ANOVA, predictor: Season, $F_{(2,\,304)} = 36.28$, $p < 0.0001$) in the early summer ($L_f = 7.71 \pm 0.10$ mm) in both rivers than the later summer ($L_f = 6.77 \pm 0.12$ mm). Results from the GLM indicated all of the spatiotemporal variables, in addition to L_f, were predictors of clutch size (GLM, $\chi^2 = 1251.6$, $p < 0.0001$, *pseudo*-$R^2 = 0.33$). After sequentially removing all interaction terms with $p > 0.05$, the final model included Tributary, Season, L_f and

an interaction between Tributary and Season (Table 3). Visual examination of the fitted clutch size vs. L_f curves indicated that Choptank females had higher clutch size than Patuxent females at a given length during the early summer months (Figure 5). These spatial differences in clutch size at a given female length appeared absent or potentially reversed during the late summer, patterns that were further evaluated by estimating clutch size and associated 95 % confidence intervals for females with L_f = 5 mm, 8.5 mm and 12 mm for most combinations of Tributary and Season (Figure 6). No 12-mm estimates were generated for late summer predictions because no gravid females with L_f > 10 mm were collected during that season (Table 1). In all cases, clutch size was higher in the early summer than the late summer at a given L_f (i.e., no overlap between pairwise 95% CI; also see Online Resource 4). Between tributaries, Choptank females had 18% higher clutch size at length during early summer but there was no difference between tributaries during the late summer (Figure 6).

Size-specific clutch size (C_{ss}) of *N. americana* differed spatiotemporally between tributaries and seasons (GLM, χ^2 =182.09, $p < 0.0001$, *pseudo*-R^2 = 0.10; Table 3). The presence of a three-way interaction (Tributary × Season × L_f, $F = 4.13$, $p = 0.04$) precluded direct interpretation of main effects in the model. Similar to C_t, GLM results for C_{ss} were evaluated by estimating C_{ss} ± 95% CI for 5-mm, 8.5-mm and 12-mm females for each combination of Tributary and Season except for 12-mm females in late summer (Figure 6). With the exception of late summer Choptank females, C_{ss} was positively related to L_f. During the early summer, Choptank C_{ss} was greater than Patuxent C_{ss} for 8.5-mm and 12-mm females but not 5-mm females. During the late summer, Choptank females showed a declining C_{ss} with increasing body size. Despite opposing trends of predicted C_{ss} with L_f among late summer Patuxent and Choptank

420 females, differences in mean predicted C_{ss} between tributaries did not exceed 95% CIs (Figure 6;
421 Online Resource 4).

422 Embryo length increased (ANOVA, $F_{2,241} = 1{,}287.10$, $p < 0.0001$) from Stage I (0.39 ±
423 0.01 mm [SE]) to Stage II (0.90 ± 0.01 mm) and finally to Stage III (1.18 ± 0.02 mm).
424 Exponential least-squares regressions of $E_l{:}C_t$ against L_f ($R^2 \geq 0.76$, $p < 0.0001$; Figure 7)
425 indicated $E_l{:}C_t$ ratios showed a consistent, but stage dependent, inverse relationship with body
426 size. Residuals of length specific $E_l{:}C_t$ ratios averaged 0.002 (0.00005 – 0.004 [95% CI])
427 mm/embryo higher (2-way ANOVA, predictor: Tributary, $F_{(1, 240)} = 23.19$, $p < 0.0001$) among
428 Choptank females than Patuxent females after accounting for embryo stage (Figure 7).
429
430 *3.4 Growth rates*
431 Modal GR_D of *N. americana* ranged from 0.009 to 0.11 mm/d and averaged 0.05 ± 0.03 mm/d
432 (SD) during the study period. Daily growth rates differed between adults and juveniles (GLM,
433 factor: Life stage, $F_{(1,21)} = 13.86$, $p = 0.003$) with juveniles growing approximately twice as fast
434 as adults (Table 4). There was no evidence of consistent differences in GR_D between tributaries
435 or seasons.
436
437 *3.5 Clutch size-environment relationships*
438 In the Patuxent River, C_{ss} was positively correlated with DO and Chl-a (Kendall rank correlation,
439 Figure 8, Table 5). In both tributaries, C_{ss} was negatively correlated with water temperature, a
440 relationship that matches results from the C_{ss} GLM that indicated C_{ss} was lower during the late
441 summer than the early summer in both systems (Figure 5). No other water quality variable
442 correlated with C_{ss} only in the Choptank River but two variables, water temperature and DO,

443 were negatively and positively (respectively) correlated with C_{ss} when data were combined
444 between tributaries.
445
446 **4. Discussion**
447 The goals of this study were to: 1) quantify growth and clutch size of *N. americana* in
448 Chesapeake Bay tributaries, 2) determine if either growth or clutch size differ spatially or
449 temporally in the study area, 3) confirm assignment of *N. americana* of both rivers to the same
450 cryptic species (ancestral lineage C), and 4) evaluate evidence of environmental drivers of clutch
451 size. The multi-pronged approach (biological, ecological, and genetic measurements) allowed us
452 to compare the growth, clutch size and population connectivity of an important omnivorous
453 consumer and prey species between two productive rivers within the Chesapeake Bay ecosystem.
454 By simultaneously assessing this suite of response variables, this project provided an opportunity
455 to test the hypothesis that *N. americana* in the Choptank River experience higher individual-level
456 clutch size and growth in that system, while also exploring the evidence that any observed
457 underlying differences in the productivity of these populations could arise from environmental
458 conditions.
459
460 *4.1 Genetic structure of mysid populations*
461 Intraspecific phylogenetic analysis of *N. americana* CO1 sequences revealed three divergent
462 lineages between the Chesapeake Bay and the St. Lawrence Estuary, indicating long-standing
463 genetic separation of the two regions and the existence of multiple cryptic lineages in *N.*
464 *americana* in the Northeast Atlantic. Previous work by Cortial et al. (2019) found a very similar
465 pattern of three, deeply-diverged lineages from samples in the St. Lawrence Estuary, the Gulf of

Maine, and a single Chesapeake Bay population. With relatively few samples from St. Lawrence Estuary (n = 17), we also recovered the two observed divergent lineages, which grouped very distinctly from the Chesapeake Bay samples in both the neighbor joining tree and RMST network. Given the percent divergence among these haplotype groups, it is possible that they represent cryptic species of *N. americana,* though additional experimental work and analysis with nuclear markers will be needed to confirm this.

Comparison of populations within each region via AMOVA and PhiSt estimation showed no evidence genetic structure or inter-population heterogeneity, which was supported by the distribution of haplotypes in the RMST networks and the neighbor joining tree topology. Within Chesapeake Bay population samples specifically, the two tributaries appeared to be very well-mixed genetically, with a homogenous distribution of haplotypes observed between the Patuxent and Choptank rivers. Based on the results of prior genetic studies for *Neomysis sp.* (e.g., Remerie et al. 2009; Cortial et al. 2019) the CO1 marker appears to provide sufficient resolution of intraspecific diversity and is also able to detect deeper divergence of interspecific diversity, i.e., potentially cryptic species or lineages. This marker has been extensively and successfully used for intraspecific population genetic analyses and identification of cryptic lineages in other zooplankton species, including copepods (Bucklin et al. 1996; Bucklin et al. 2000; Chen and Hare 2011; Höring et al. 2017; Plough et al. 2018). For the present study, the primary goal of the genetic analyses was to examine the possibility that cryptic genetic lineages or other strong genetic breaks between Chesapeake Bay populations could explain the observed clutch size differences between samples the two tributaries. While sample sizes for the Chesapeake populations were relatively small (n = 15 in Patuxent River, n = 19 in Choptank River), the genetic results provide no evidence for the presence of cryptic lineages or any substantial genetic

structure over the scale of 10s of km in Chesapeake Bay and thus genetic differences do not explain the observed differences in clutch size between the two tributaries. Nevertheless, power to detect fine-scale genetic structure may be limited with mtDNA in general (e.g., Teske et al. 2018) and Fratini et al. (2016) suggested that larger population sizes and exhaustive geographic sampling may be needed to detect subtler patterns of genetic structure. Additional genetic surveys of *N. americana* using higher resolution nuclear markers (e.g. genome-wide SNPs) should be conducted to confirm these findings, and to understand the extent to which gene flow is occurring among other *N. americana* populations within Chesapeake Bay.

4.2 Spatial, temporal and environmental patterns in clutch size

In this study, clutch size in Chesapeake Bay *N. americana* ranged from 1 to 71 and averaged 20 ± 13 (SD) embryos per female across all sampling periods and locations, values that are generally comparable than those reported elsewhere (Passamaquoddy Bay, ME: 1~77, Pezzack and Corey 1979; Maryland Coastal Bays: 1~75, Mayor et al. 2017; e.g., St. Lawrence Estuary, Canada: 5–63, Bouchard and Winkler 2018). Generally speaking, larger females produced more embryos, the only exception being Choptank River females in the late summer. Other studies have observed a similar non-linear decline in clutch size among the largest females in a cohort, possibly reflecting senescence-associated reduction in reproductive output among the largest and putatively oldest, females (Bouchard and Winkler 2018). It is more difficult to compare our estimates and analysis of C_{ss} because size-specific clutch size is not typically reported beyond the fitting of linear or log-linear models that seek to predict clutch size as a function of body length. Still, using linear regression, other studies have reported C_{ss} ranging from 0.9 to 4.6 embryos per mm female length (0.9–2.3 embryos/mm, Wigley and Burns 1971;

512 4.6 embryos/mm, Mayor et al. 2017), very similar to our average C_{ss} of 2.6 ± 3.1 (SD)
513 embryos/mm.

514 Spatially, clutch size was higher in the Choptank than the Patuxent River during the
515 spring, despite Choptank female body size averaging 0.53 ± 0.2 (SE) mm less than Patuxent
516 females during that same period (Tukey post-hoc test, t =2.62, p = 0.045) and a lack of
517 discernible genetic differences between populations. Patterns in C_{ss} were similar, albeit less
518 consistent, with Choptank C_{ss} values tending to be higher in the early summer followed by a shift
519 toward slightly higher values in the Patuxent River in the late summer at the very largest body
520 sizes. These results suggest winter and early spring conditions in the Choptank favored greater
521 clutch size at size for the overwintering cohort of females although it is not clear precisely what
522 conditions led to this outcome. The quality and (or) quantity of food, as well as differences in
523 local environmental conditions are both possible factors.

524 Given the importance of body size in determining predation risk among crustaceans
525 (Maszczyk and Brzezinski 2018), the consistently higher ratio of embryo length to clutch size
526 after accounting for female size (E_l:C_t ratio) in Choptank females indicates that newly released
527 larvae may experience lower mortality rates than conspecific larvae from females with a similar
528 clutch size in the Patuxent River. Pezzack and Corey (1979) examined egg and larvae sizes and
529 found that the size of embryos was more variable within than between individual when compared
530 among body size, brood size, or season. While we were unable to evaluate seasonal effects, we
531 did find consistent effects of brood size, female size, larval stage, and population on relative
532 embryo size. Some of these trends have been observed in other marine peracaridan crustaceans
533 (Johnson et al. 2001) but very little information is available on the direct causes and ecological
534 implications of variable embryo size at release for mysids. In general, larger body size allows for

quicker reaction times, a key component of predator avoidance and prey capture, and can also confer starvation resistance relative to smaller individuals (Maszczyk and Brzezinski 2018). Cannibalism, common among mysid taxa and shown to affect population dynamics (e.g., *Americamysis bahia*, Grear et al. 2011), is size-dependent in gape-limited predators such as mysids and may be reduced among larvae with relatively larger body size at release.

Local differences in the seasonal availability of food, whether due to differences in absolute abundance or phenological shifts in the timing of population growth or reproductive cycles, could both contribute to the spatial and temporal patterns in clutch size observed in this study. While *N. americana* appear to selectively feed on smaller zooplankton prey such as rotifers, veliger-stage bivalve larvae, and copepod nauplii when available, the species is capable of consuming a wide variety of plant, animal, and detrital material (Fulton 1982; Winkler et al. 2003; Winkler et al. 2007). Experimental studies have demonstrated that the productivity, growth, and survival of other mysid species can respond to changes in the composition of zooplankton prey (e.g., *Leptomysis* sp., Domingues et al. 2000; *Mysis mixta*, Lehtiniemi et al. 2002). Observational data suggest *N. americana* population dynamics are similarly responsive to changes in food availability. In the St. Lawrence Estuary, *N. americana* clutch size was positively related to ambient chlorophyll-*a* and suspended particulate organic matter concentrations (Bouchard and Winkler 2018). Using stable isotope data, Quillen et al. (2022) found that *N. americana* diet consisted of ~25% benthic-derived food in the Choptank River as compared to ~8% in the Patuxent River in 2018 and 2019. In that same study, Choptank *N. americana* that assimilated more benthic food also had a higher tissue proxy for lipid content (C:N ratio) than those in the Patuxent River (Quillen et al. 2022). If the increased lipid storage in the Choptank River mysids was available for egg production, it could explain the higher clutch

size observed in Choptank River females in this study during the same period of time (Gorokhova and Hansson 2000). Unfortunately, data on food availability from the Patuxent and Choptank rivers are not available for this study, but future experiments exploring the links between food availability and *N. americana* population dynamics could elucidate how trophic interactions ultimately affect productivity of this species.

A number of studies have documented environmental conditions that correlate with *N. americana* relative abundance (Schiariti et al. 2006; Mayor and Chigbu 2018; Espinosa et al. 2019), but fewer have looked at the potential role of environmental conditions on clutch size. In Chesapeake Bay, the negative correlation between water temperature and C_{ss} aligns with the results from the seasonal clutch size analysis that showed smaller body size and lower clutch size in the late summer. As mentioned above, Bouchard and Winkler (2018) found a positive relationship between clutch size and two food proxies in the St. Lawrence Estuary but they did not find a relationship between clutch size and temperature or salinity. Although not specifically analyzed, numerous studies have also documented an apparent negative relationship between water temperature and clutch size, often discussed as a decline in mean clutch size of females belonging to overwintering cohorts relative to summer cohorts (Pezzack and Corey 1979; e.g., Mayor et al. 2017). This suggests a negative correlation between cohort fecundity and water temperature, but most of these studies did not specifically account for body size, which also typically declines across the same cohorts. The declines in C_{ss} with increasing temperature observed here suggest *N. americana* may experience reduced individual-level productivity in some areas of Chesapeake Bay under a warming climate. Whether individual-level reductions in clutch size would ultimately affect fecundity and population-level productivity depends on how individual growth and survival also covary with temperature.

581 The positive correlations between C_{ss} and both DO and Chl-a in the Patuxent support the
582 hypothesis that water quality and food availability affect *N. americana* production. The absence
583 of a relationship between these variables in the Choptank River may be due to differences in the
584 range of conditions present in that river. Specifically, the range of average near-bottom DO and
585 Chl-a values were narrower in the Choptank, lacking the very low and very high values observed
586 in the Patuxent River (Figure 9). While hypoxia effects on fecundity of *N. americana* are
587 unknown, experimental work with the congener *Neomysis awatschensis* documented a 94 %
588 decline in juvenile production from 8.5 mg/L (control) to 4 mg/L, well above the 2 mg/L
589 threshold typically used to define hypoxia (Wang et al. 2021). If *N. americana* juvenile
590 production is similarly sensitive to ambient oxygenation, vertical migration away from bottom
591 waters with lethal DO concentrations may still expose females to intermediate DO ranges that
592 impair production. Quantifying DO-clutch size relationships for *N. americana* under realistic
593 temperature and salinity conditions using flexible non-linear modelling approaches (e.g.,
594 generalized additive models; Wood 2017) is a critical next step in understanding the influence of
595 summer hypoxia on this species.

596 Periods of chronic seasonal hypoxia in the Patuxent River are associated with broad shifts
597 in planktonic community composition, including reduced copepod (adult, copepodite, and
598 nauplius stages) and fish (egg and larval stages) abundance, as well as increased gelatinous
599 zooplankton abundance (Keister et al. 2000). At the community level, changes in trophic
600 interactions within the water column, primarily due to increased gelatinous zooplankton predator
601 abundance and altered predator-prey encounter rates arising from changing access to deep water
602 habitats, have been proposed as mechanisms contributing to these community changes (Breitburg
603 et al. 2003; Kolesar et al. 2010). Quillen et al. (2022) hypothesized that avoidance of hypoxic

deep waters in the Patuxent River led to a greater reliance of *N. americana* on pelagic trophic pathways, leading to decoupling of mysids from benthic trophic resources and making them more reliant on pelagic resources. The positive correlation of clutch size with Chl-a concentrations in the Patuxent River observed in this study supports that hypothesis. In the Choptank River, access to bottom habitats should not be constrained by hypoxia, therefore benthic trophic resources should be more available and reproductive output no longer coupled as tightly to the availability of pelagic resources. Taken together, it appears that the productivity of *N. americana* is sensitive to local water quality conditions and, in the presence of hypoxic bottom waters, becomes increasingly reliant on the availability of pelagic resources. The availability of pelagic trophic resources, generally dominated by recently fixed carbon (i.e., phytoplankton), tends to be more seasonal and variable than benthic trophic resource pools which are fueled by inputs of both living and detrital organic carbon. This suggests that exclusion of *N. americana* from benthic areas due to recurrent seasonal hypoxia in coastal areas could affect the stability and productivity of these populations (Rooney et al. 2006; McCann and Rooney 2009; McMeans et al. 2015).

4.3 Neomysis americana growth in Chesapeake Bay

Growth rates of *N. americana* in Chesapeake Bay are similar to those reported in other coastal systems. In this study, juvenile growth rates were more than double adult growth rates with a mean difference in rates, ΔGR_D (juvenile GR_D – adult GR_D), of 0.034 mm/d. This ontogenetic difference generally aligns with observations by Viñas et al. (2005) for an invasive population of *N. americana* in Samborombón Bay, Argentina (ΔGR_D = 0.009–0.024 mm/d) and a higher latitude North American system (St. Lawrence Estuary, Canada ΔGRD = 0.039–0.083 mm/d,

627 Bouchard and Winkler 2018). Seasonal differences in growth rates among cohorts in our study
628 indicated slower growth by the late summer cohort, a pattern that was also observed in South
629 America but not in Canada (Viñas et al. 2005; Bouchard and Winkler 2018). *Neomysis*
630 *americana* displayed an opposite seasonal growth pattern in Passamaquoddy Bay, with summer
631 cohort growth rates more than twice that of spring growth rates (Pezzack and Corey 1979). The
632 dissimilar growth pattern in Passamaquoddy Bay is likely due to local conditions such as
633 primary-secondary production cycles rather than broad geographic differences in thermal regime
634 because the Pezzack and Corey (1979) study occurred at a latitude intermediate between the
635 Bouchard and Winkler (2018) St. Lawrence Estuary study and this study.

636 Contrary to our initial hypothesis, we did not observe a difference in growth rates
637 between the Choptank and Patuxent rivers. The absence of a difference in growth rate between
638 these rivers is interesting given the between-river differences in clutch size and C_{ss} observed in
639 this study and the differences in trophic resource use and lipid stores between rivers during the
640 same period that were observed in a previous study (Quillen et al. 2022). The fact that *N.*
641 *americana* females were able to maintain similar growth trajectories despite achieving different
642 levels of reproductive output suggests that the range of optimal conditions supporting somatic
643 and reproductive growth differ for this species. Wang et al. (2021) observed similar results in
644 laboratory experiments using *N. awatschensis*, in which daily growth rates were not sensitive to
645 hypoxia treatments despite reductions in tissue fatty acid storage, survival, and clutch size. Using
646 Patuxent River *N. americana*, Chapina et al. (2020) showed that basal metabolic rates of gravid
647 *N. americana* females were higher than those of non-gravid females and sexually mature males.
648 Considering our observations, we hypothesize that the combination of environmental conditions
649 (e.g., near-bottom dissolved oxygen concentrations) and trophic resources in the Choptank River

were better able to meet the elevated metabolic requirements of gravid *N. americana*, leading to higher clutch size and larger relative embryo size in that system.

4.4 Conclusions

Mysid population dynamics are complex and sensitive to environmental and biological effects on growth, survival, maturation, and fecundity (Grear et al. 2011). We found evidence that spatial and temporal patterns in clutch size are better explained by local environmental conditions, rather than genetic differentiation, in Chesapeake Bay tributaries. Furthermore, this study highlights the spatiotemporal variability in female size, clutch size, and larval size of *N. americana* that exist in the region. In Chesapeake Bay and elsewhere, efforts to remediate water quality through nutrient, sediment, and contaminant reductions often focus on chemical, biogeochemical, and physiochemical indicators of success. Here, we have shown that mysid clutch size metrics may provide a useful biological indicator for evaluating community response to changes in water quality. Given the widely documented importance of mysids in coastal food webs, future work that builds understanding of mysid-environment relationships, as well as insights into population dynamics, seasonal migrations, and predator-prey interactions, will provide valuable information for natural resource managers.

Acknowledgments

We thank Captain Richie Long, Katie Lankowicz, Alec Armstrong, Nicholas Johnson, Benjamin Lee, Alexandra Fireman, and Fiona G.N. Woodland for help in the field. Benjamin Lee provided assistance preparing and processing genetics samples. Drs. Hongsheng Bi and Elizabeth North provided suggestions on earlier versions of this study. We thank Drs. Michael Allen and Fredrika Moser for their support. This project was funded by Maryland Sea Grant award #07-5-25839, National Science Foundation award OCE-2023349 (UMCES) and OCE-1756244 (Maryland Sea Grant REU Program), and Chesapeake Biological Laboratory.

Literature cited

Aktas C. 2023. *haplotypes*: Manipulating DNA Sequences and Estimating Unambiguous Haplotype Network with Statistical Parsimony. *R* package version 1.1.3.1. Link: https://cran.r-project.org/web/packages/haplotypes/haplotypes.pdf

Akiyama, S., M. Ueno, and Y. Yamashita. 2015. Population dynamics and reproductive biology of the mysid *Orientomysis japonica* in Tango Bay, Japan. *Plankton and Benthos Research* 10: 121-131.

Bouchard, L., and G. Winkler. 2018. Life cycle, growth and reproduction of Neomysis americana in the St. Lawrence estuarine transition zone. *Journal of Plankton Research* 40: 693-707.

Breitburg, D., L.A. Levin, A. Oschlies, M. Gregoire, F.P. Chavez, D.J. Conley, V. Garcon, D. Gilbert, D. Gutierrez, K. Isensee, G.S. Jacinto, K.E. Limburg, I. Montes, S.W.A. Naqvi, G.C. Pitcher, N.N. Rabalais, M.R. Roman, K.A. Rose, B.A. Seibel, M. Telszewski, M. Yasuhara, and J. Zhang. 2018. Declining oxygen in the global ocean and coastal waters. *Science* 359: eaam7240.

Breitburg, D.L., A. Adamack, K.A. Rose, S.E. Kolesar, M.B. Decker, J.E. Purcell, J.E. Keister, and J.H. Cowan. 2003. The pattern and influence of low dissolved oxygen in the Patuxent River, a seasonally hypoxic estuary. *Estuaries* 26: 280-297.

Buchheister, A., and R.J. Latour. 2015. Diets and trophic-guild structure of a diverse fish assemblage in Chesapeake Bay, U.S.A. *Journal of Fish Biology* 86: 967-992.

Bucklin, A., O.S. Astthorsson, A. Gislason, L.D. Allen, S.B. Smolenack, and P.H. Wiebe. 2000. Population genetic variation of *Calanus finmarchicus* in Icelandic waters: preliminary

698 evidence of genetic differences between Atlantic and Arctic populations. *ICES Journal of*
699 *Marine Science* 57: 1592-1604.

700 Bucklin, A., T.C. LaJeunesse, E. Curry, J. Wallinga, and K. Garrison. 1996. Molecular diversity
701 of the copepod, *Nannocalanus minor*: genetic evidence of species and population
702 structure in the North Atlantic Ocean. *Journal of Marine Research* 54: 285-310.

703 Chapina, R.J., C.L. Rowe, and R.J. Woodland. 2020. Metabolic rates of *Neomysis americana*
704 (Smith, 1873)(Mysida: Mysidae) from a temperate estuary vary in response to summer
705 temperature and salinity conditions. *The Journal of Crustacean Biology* 40: 450-454.

706 Chen, G., and M.P. Hare. 2011. Cryptic diversity and comparative phylogeography of the
707 estuarine copepod *Acartia tonsa* on the US Atlantic coast. *Molecular Ecology* 20: 2425-
708 2441.

709 Cortial, G., R. Woodland, R. Lasley-Rasher, and G. Winkler. 2019. Phylogeography of *Neomysis*
710 *americana* (Crustacea, Mysida), focusing on the St. Lawrence system. *Journal of*
711 *Plankton Research* 41: 723-739.

712 Cottenie, K. 2005. Integrating environmental and spatial processes in ecological community
713 dynamics. *Ecology Letters* 8: 1175-1182.

714 Domingues, P., R. Forés, P. Turk, P. Lee, and J.P. Andrade. 2000. Mysid culture: lowering costs
715 with alternative diets. *Aquaculture Research* 31: 719-728.

716 Donnelly, J., D. Stickney, and J. Torres. 1993. Proximate and elemental composition and energy
717 content of mesopelagic crustaceans from the Eastern Gulf of Mexico. *Marine Biology*
718 115: 469-480.

719 Elliott, M., and A.K. Whitfield. 2011. Challenging paradigms in estuarine ecology and
720 management. *Estuarine, Coastal and Shelf Science* 94: 306-314.

721 Espinosa, N., D. Calliari, and L. Rodríguez-Graña. 2019. Life history, population structure and
722 environmental modulation of *Neomysis americana* (Mysinae) in an intermittently open
723 coastal lagoon of the South West Atlantic. *Estuarine, Coastal and Shelf Science* 223:
724 129-137.

725 Excoffier, L., P.E. Smouse, and J. Quattro. 1992. Analysis of molecular variance inferred from
726 metric distances among DNA haplotypes: application to human mitochondrial DNA
727 restriction data. *Genetics* 131: 479-491.

728 Fisher, T., J.I.D. Hagy, W. Boynton, and M. Williams. 2006. Cultural eutrophication in the
729 Choptank and Patuxent estuaries of Chesapeake Bay. *Limnology and Oceanography* 51:
730 435-447.

731 Fockedey, N., J. Mees, M. Vangheluwe, T. Verslycke, C.R. Janssen, and M. Vincx. 2005.
732 Temperature and salinity effects on post-marsupial growth of *Neomysis integer*

(Crustacea: Mysidacea). *Journal of Experimental Marine Biology and Ecology* 326: 27-47.

Fratini, S., L. Ragionieri, T. Deli, A. Harrer, I.A. Marino, S. Cannicci, L. Zane, and C.D. Schubart. 2016. Unravelling population genetic structure with mitochondrial DNA in a notional panmictic coastal crab species: sample size makes the difference. *BMC Evolutionary Biology* 16: 1-15.

Froneman, P.W. 2001. Feeding ecology of the mysid, Mesopodopsis wooldridgei, in a temperate estuary along the eastern seaboard of South Africa. *Journal of Plankton Research* 23: 999-1008.

Fulton, R.S. 1982. Predatory feeding of two marine mysids. *Marine Biology* 72: 183-191.

Gayanilo, F.C.J., P. Sparre, and D. Pauly. 2005. FAO-ICLARM Stock Assessment Tools II (FiSAT II). Revised version. User's guide.

Geller, J., C. Meyer, M. Parker, and H. Hawk. 2013. Redesign of PCR primers for mitochondrial cytochrome c oxidase subunit I for marine invertebrates and application in all-taxa biotic surveys. *Molecular ecology resources* 13: 851-861.

Gorokhova, E., and S. Hansson. 2000. Elemental composition of *Mysis mixta* (Crustacea, Mysidacea) and energy costs of reproduction and embryogenesis under laboratory conditions. *Journal of experimental marine Biology and Ecology* 246: 103-123.

Grear, J.S., D.B. Horowitz, and R. Gutjahr-Gobell. 2011. Mysid population responses to resource limitation differ from those predicted by cohort studies. *Marine Ecology Progress Series* 432: 115-123.

Heard, R.W., W.W. Price, D.M. Knott, R.A. King, and D.M. Allen. 2006. *A taxonomic guide to the mysids of the South Atlantic Bight*. National Marine Fisheries Service, NOAA: Scientific Publications Office, National Marine Fisheries Service, NOAA.

Hines, A.H., A.M. Haddon, and L.A. Wiechert. 1990. Guild structure and foraging impact of blue crabs and epibenthic fish in a subestuary of Chesapeake Bay. *Marine Ecology Progress Series*.

Höring, F., A. Cornils, H. Auel, M. Bode, and C. Held. 2017. Population genetic structure of *Calanoides natalis* (Copepoda, Calanoida) in the eastern Atlantic Ocean and Benguela upwelling system. *Journal of Plankton Research* 39: 618-630.

Ihde, T.F., E.D. Houde, C.F. Bonzek, and E. Franke. 2015. Assessing the Chesapeake Bay forage base: Existing data and research priorities, ed. S.a.T.A. Committee, 198. Edgewater, MD: Chesapeake Bay Program Scientific and Technical Advisory Committee.

Johnson, W.S., M. Stevens, and L. Watling. 2001. Reproduction and development of marine peracaridans. In *Advances in Marine Biology*, 105-260: Academic Press.

768 Jumars, P.A. 2007. Habitat coupling by mid-latitude, subtidal, marine mysids: Import-subsidised
769 omnivores. *Oceanography and Marine Biology* 45: 89-138.

770 Keister, J.E., E.D. Houde, and D.L. Breitburg. 2000. Effects of bottom-layer hypoxia on
771 abundances and depth distributions of organisms in Patuxent River, Chesapeake Bay.
772 *Marine Ecology Progress Series* 205: 43-59.

773 Kemp, W.M., W.R. Boynton, J.E. Adolf, D.F. Boesch, W.C. Boicourt, G. Brush, J.C. Cornwell,
774 T.R. Fisher, P.M. Glibert, J.D. Hagy, L.W. Harding, E.D. Houde, D.G. Kimmel, W.D.
775 Miller, R.I.E. Newell, M.R. Roman, E.M. Smith, and J.C. Stevenson. 2005.
776 Eutrophication of Chesapeake Bay: Historical trends and ecological interactions. *Marine*
777 *Ecology Progress Series* 303: 1-29.

778 Kennish, M.J. 2002. Environmental threats and environmental future of estuaries. *Environmental*
779 *Conservation* 29: 78-107.

780 Kolesar, S.E., D.L. Breitburg, J.E. Purcell, and M.B. Decker. 2010. Effects of hypoxia on
781 *Mnemiopsis leidyi,* ichthyoplankton and copepods: clearance rates and vertical habitat
782 overlap. *Marine Ecology Progress Series* 411: 173-188.

783 Kumar, S., K. Tamura, and M. Nei. 1994. MEGA: molecular evolutionary genetics analysis
784 software for microcomputers. *Bioinformatics* 10: 189-191.

785 Larsson, A. 2014. AliView: a fast and lightweight alignment viewer and editor for large datasets.
786 *Bioinformatics* 30: 3276-3278.

787 Lehtiniemi, M., M. Viitasalo, and H. Kuosa. 2002. Diet composition influences the growth of the
788 pelagic mysid shrimp, *Mysis mixta* (Mysidacea). *Boreal environment research* 7: 121.

789 Liquete, C., C. Piroddi, E.G. Drakou, L. Gurney, S. Katsanevakis, A. Charef, and B. Egoh. 2013.
790 Current status and future prospects for the assessment of marine and coastal ecosystem
791 services: a systematic review. *PloS one* 8: e67737.

792 Lotze, H.K., H.S. Lenihan, B.J. Bourque, R.H. Bradbury, R.G. Cooke, M.C. Kay, S.M. Kidwell,
793 M.X. Kirby, C.H. Peterson, and J.B.C. Jackson. 2006. Depletion, degradation, and
794 recovery potential of estuaries and coastal seas. *Science* 312: 1806-1809.

795 Maszczyk, P., and T. Brzezinski. 2018. Body size, maturation size, and growth rate of
796 crustaceans. *The natural history of the Crustacea* 5: 35-65.

797 Mauchline, J. 1980. *The biology of mysids and euphausiids*: Academic Press.

798 Mayor, E., P. Chigbu, J. Pierson, and V.S. Kennedy. 2017. Composition, abundance, and life
799 history of mysids (Crustacea: Mysida) in the coastal lagoons of MD, USA. *Estuaries and*
800 *Coasts* 40: 224-234.

Mayor, E.D., and P. Chigbu. 2018. Mysid shrimp dynamics in relation to abiotic and biotic factors in the coastal lagoons of Maryland, Mid-West Atlantic, USA. *Marine Biology Research* 14: 621-636.

McCann, K.S., and N. Rooney. 2009. The more food webs change, the more they stay the same. *Philosophical Transactions of the Royal Society B: Biological Sciences* 364: 1789-1801.

McMeans, B.C., K.S. McCann, M. Humphries, N. Rooney, and A.T. Fisk. 2015. Food web structure in temporally-forced ecosystems. *Trends in Ecology & Evolution* 30: 662-672.

Nei, M., and S. Kumar. 2000. *Molecular evolution and phylogenetics*: Oxford University Press, USA.

Nyström, M., A.V. Norström, T. Blenckner, M. de la Torre-Castro, J.S. Eklöf, C. Folke, H. Österblom, R.S. Steneck, M. Thyresson, and M. Troell. 2012. Confronting feedbacks of degraded marine ecosystems. *Ecosystems* 15: 695-710.

Pagenkopp Lohan, K.M., R. Aguilar, R. DiMaria, K. Heggie, T.D. Tuckey, M.C. Fabrizio, and M.B. Ogburn. 2023. Juvenile Striped Bass consume diverse prey in Chesapeake Bay tributaries. *Marine and Coastal Fisheries* 15: e10259.

Paradis, E. 2010. pegas: an R package for population genetics with an integrated–modular approach. *Bioinformatics* 26: 419-420.

Paradis, E. 2018. Analysis of haplotype networks: The randomized minimum spanning tree method. *Methods in Ecology and Evolution* 9: 1308-1317.

Paul, S., and G.P. Closs. 2014. Effects of salinity and food quality on the growth of sub-adult mysids of *Tenagomysis* spp.: a laboratory study. *Aquatic ecology* 48: 229-235.

Pezzack, D.S., and S. Corey. 1979. Life history and distribution of *Neomysis americana* (Smith) (Crustacea, Mysidacea) in Passamaquoddy Bay. *Canadian Journal of Zoology-Revue Canadienne De Zoologie* 57: 785-793.

Plough, L., C. Fitzgerald, A. Plummer, and J. Pierson. 2018. Reproductive isolation and morphological divergence between cryptic lineages of the copepod Acartia tonsa in Chesapeake Bay. *Marine Ecology Progress Series* 597: 99-113.

Quillen, K., N. Santos, J.M. Testa, and R.J. Woodland. 2022. Coastal hypoxia reduces trophic resource coupling and alters niche characteristics of an ecologically dominant omnivore. *Food Webs*: e00252.

Remerie, T., A. Vierstraete, P.H. Weekers, J.R. Vanfleteren, and A. Vanreusel. 2009. Phylogeography of an estuarine mysid, *Neomysis integer* (Crustacea, Mysida), along the north-east Atlantic coasts. *Journal of Biogeography* 36: 39-54.

Rooney, N., K. McCann, G. Gellner, and J.C. Moore. 2006. Structural asymmetry and the stability of diverse food webs. *Nature* 442: 265-269.

836 Schiariti, A., A.D. Berasategui, D.A. Giberto, R.A. Guerrero, E.M. Acha, and H.W. Mianzan.
837 2006. Living in the front: *Neomysis americana* (Mysidacea) in the Rio de la Plata estuary,
838 Argentina-Uruguay. *Marine Biology* 149: 483-489.

839 Schneider, C.A., W.S. Rasband, and K.W. Eliceiri. 2012. NIH Image to ImageJ: 25 years of
840 image analysis. *Nature Methods* 9: 671-675.

841 Tattersall, W.M. 1951. The Mysidacea of the United States National Museum. In Bulletin of the
842 United States National Museum, #201, 292 pgs. Washington, DC: Smithsonian
843 Institution.

844 Teske, P.R., T.R. Golla, J. Sandoval-Castillo, A. Emami-Khoyi, C.D. Van der Lingen, S. Von
845 der Heyden, B. Chiazzari, B. Jansen van Vuuren, and L.B. Beheregaray. 2018.
846 Mitochondrial DNA is unsuitable to test for isolation by distance. *Scientific reports* 8:
847 8448.

848 Toda, H., S. Nishizawa, M. Takahashi, and S. Ichimura. 1983. Temperature control on the post-
849 embryonic growth of *Neomysis intermedia Czerniawsky* in a hypereutrophic temperate
850 lake. *Journal of Plankton Research* 5: 377-392.

851 Viñas, M.D., F.C. Ramírez, and H.W. Mianzan. 2005. Annual population dynamics of the
852 opossum shrimp *Neomysis americana* Smith, 1873 (Crustacea, Mysidacea) from an
853 estuarine sector of the Argentine Sea. *Scientia Marina* 69: 493-502.

854 Wang, Q.-n., X.-d. Li, T. Yan, J.-j. Song, R.-c. Yu, and M.-j. Zhou. 2021. Detrimental impact of
855 hypoxia on the mortality, growth, reproduction, and enzyme activities of planktonic
856 mysid *Neomysis awatschensis*. *Aquatic Ecology* 55: 849-859.

857 Wigley, R., and B. Burns. 1971. Distribution and biology of mysids (Crustracea, Mysidacea)
858 from the Atlantic coast of the United States in the NMFS Woods Hole collection. *Fish.*
859 *Bull.* 69: 717-746.

860 Winkler, G., J.J. Dodson, N. Bertrand, D. Thivierge, and W.F. Vincent. 2003. Trophic coupling
861 across the St. Lawrence River estuarine transition zone. *Marine Ecology Progress Series*
862 251: 59-73.

863 Winkler, G., and W. Greve. 2002. Laboratory studies of the effect of temperature on growth,
864 moulting and reproduction in the co-occurring mysids *Neomysis integer* and *Praunus*
865 *flexuosus*. *Marine Ecology Progress Series* 235: 177-188.

866 Winkler, G., C. Martineau, J.J. Dodson, W.F. Vincent, and L.E. Johnson. 2007. Trophic
867 dynamics of two sympatric mysid species in an estuarine transition zone. *Marine Ecology*
868 *Progress Series* 332: 171-187.

869 Wood, S.N. 2017. *Generalized additive models: an introduction with R*. Chapman and
870 Hall/CRC: Chapman and Hall/CRC.

871 Zagursky, G., and R.J. Feller. 1985. Macrophyte detritus in the winter diet of the estuarine
872 mysid, *Neomysis americana*. *Estuaries* 8: 355-362.
873

Tables

Table 1. Summary of *Neomysis americana* samples used in the clutch size and growth rate components of this study, including sample size (n) for all analyses, average ± SD of clutch size (C_t, embryos per individual), size-specific clutch size (C_{ss}, embryos per unit body length), and average length (L, with minimum and maximum) of *N. americana* used in growth calculations.

			Clutch size			Growth	
				C_t	C_{ss}		L
Tributary	Year	Month	n	(embryos / ind.)	(embryos / mm)	n	(min-max)
Choptank	2018	May	50	25.08 ± 13.99	3.21 ± 1.22	202	4.9 (1.2 – 13.5)
		June	7	14.71 ± 7.36	2.26 ± 0.90	148	5.3 (1.5 – 10.3)
		July		.	.	156	4.8 (1.4 – 8.0)
		August		.	.	165	2.4 (0.6 – 8.9)
		September	55	12.29 ± 3.62	2.01 ± 0.57	184	3.2 (0.7 – 8.3)
	2019	May	25	32.68 ± 16.86	4.07 ± 1.70	.	.
		August	14	7.29 ± 3.41	1.07 ± 0.59	.	.
		September	11	15.36 ± 10.6	1.98 ± 1.05	.	.
Patuxent	2018	May	60	26.98 ± 14.07	3.32 ± 1.57	137	5.4 (1.3 – 12.9)
		June	10	12.8 ± 7.30	1.89 ± 0.97	119	4.4 (1.1 – 9.9)
		July		.	.	38	3.8 (1.3 – 7.3)
		August	19	12.58 ± 9.38	1.65 ± 1.04	61	3.6 (0.7 – 9.4)
		September	6	9.00 ± 5.29	1.47 ± 0.61	15	3.1 (0.9 – 7.8)
	2019	May	25	23.04 ± 8.96	2.82 ± 1.11	.	.
		September	25	16.72 ± 5.85	2.37 ± 0.83	.	.

Table 2. Genetic diversity metrics among *Neomysis americana* populations. *n* is the sample size of each population or population grouping, *h* is Haplotype diversity (Nei 1987), and π is nucleotide diversity (Nei and Li 1979). *The St. Lawrence-sub sample (*n* = 15) is a subsample of all St. Lawrence Estuary individuals, not including the two divergent haplotypes (STL-ES-8, STL-MTZ-5) representing the 3rd cryptic lineage.

Population	*n*	*h*	π
Chesapeake Bay	34	0.9679 (0.0004)	0.0059 (0.00001)
Patuxent River	15	0.9810 (0.0006)	0.0052 (0.00001)
Choptank River	19	0.9649 (0.0011)	0.0064 (0.00001)
St. Lawrence Estuary	17	0.9191 (0.0030)	0.0109 (0.00004)
*St. Lawrence-sub**	15	0.8952 (0.0046)	0.0030 (0.000004)
Marine-transition (STL-MTZ)	10	0.7778 (0.0183)	0.0103 (0.00004)
Estuarine site (STL-ES)	7	0.9523 (0.0059)	0.0132 (0.00006)

Table 3. Generalized linear model results of clutch size (C_t), size-specific clutch size (C_{ss}) and daily growth rate (GR_D) of *Neomysis americana*. Model terms (Tributary [Trib], Season, female body length L_f) are from final versions of each model following sequential removal of interaction terms with p-values > 0.05 (all main effects retained in final version regardless of significance). F-test denominator degrees of freedom (df) determined by Satterthwaite approximation.

	C_t				C_{ss}				GR_D			
Model terms	SSQ	*df*	*F*-stat.	*p*	SSQ	*df*	*F*-stat.	*p*	SSQ	*df*	*F*-stat.	*p*
Tributary	29.41	1	8.17	0.004	0.83	1	0.60	0.44	0.0005	1	0.81	0.38
Life stage[1]	-	-	-	-	-	-	-	-	0.0079	1	14.04	0.0001
L_f	600.53	1	166.93	<0.0001	40.35	1	29.28	<0.0001	-	-	-	-
Season	194.84	1	54.16	<0.0001	2.97	1	2.16	0.14	0.0011	1	1.92	0.18
Trib× L_f	-	-	-	-	2.42	1	1.76	0.19	-	-	-	-
Trib×Season	15.78	1	4.39	0.04	4.34	1	3.15	0.08	-	-	-	-
L_f ×Season	-	-	-	-	8.14	1	5.91	0.02	-	-	-	-
Trib× L_f ×Season	-	-	-	-	5.69	1	4.13	0.04	-	-	-	-
Residuals	*1086.41*	*302*			*412.04*	*299*			*0.014*	*25*		

[1] Life stage was only included as a potential predictor in GR_D models

Table 4. Least-squares means (LSM) estimates of *Neomysis americana* daily growth rates (GR_D) with standard error (SE) for main effects from a multifactor ANOVA. Differences between predicator levels at $\alpha = 0.05$ are denoted as *.

Predictor	Level	GR_D (mm/d)	SE
Life stage *	Juvenile	0.064	0.006
	Adult	0.030	0.007
River	Choptank	0.051	0.006
	Patuxent	0.043	0.006
Season	Early	0.053	0.006
	Late	0.041	0.007
	Overall	*0.052*	*0.005*

Table 5. Kendal rank correlation analysis of *Neomysis americana* size-specific clutch size (C_{ss}, embryos / mm female length) and bottom water quality variables: chlorophyll-a (Chl-a), dissolved oxygen concentration (DO), water temperature (WTemp), and salinity. Correlations between C_{ss} and environmental variables shown for each river (Patuxent, Choptank) and combined across rivers (Total).

	Patuxent			Choptank			Total		
Variable	τ	z	p	τ	z	p	τ	z	p
Chl-a (µg/L)	0.59	2.38	0.02	-0.16	-0.68	0.5	0.13	0.96	0.34
DO (mg/L)	0.56	2.71	0.007	0.34	1.55	0.12	0.32	2.3	0.02
WTemp (°C)	-0.4	-1.94	0.05	-0.65	-3.02	0.003	-0.51	-3.68	0.0002
Salinity	-0.26	-1.16	0.24	0.07	0.31	0.76	-0.06	-0.42	0.67

Figures

Figure 1. Maps of the Patuxent (A, left) and Choptank (B, right) rivers showing mysid collection stations (square symbols) and long-term water quality sampling locations (Chesapeake Bay Program [CBP] Water Quality Monitoring Program [data.chesapeakebay.net/WaterQuality], circle [tidal fresh-oligohaline stations: TF1.5, ET5.1] and triangle [mesohaline stations: LE1.1, ET5.2] symbols). Inset: Map of Chesapeake Bay, USA, showing locations of each river (PAX, CHOP) within the Bay.

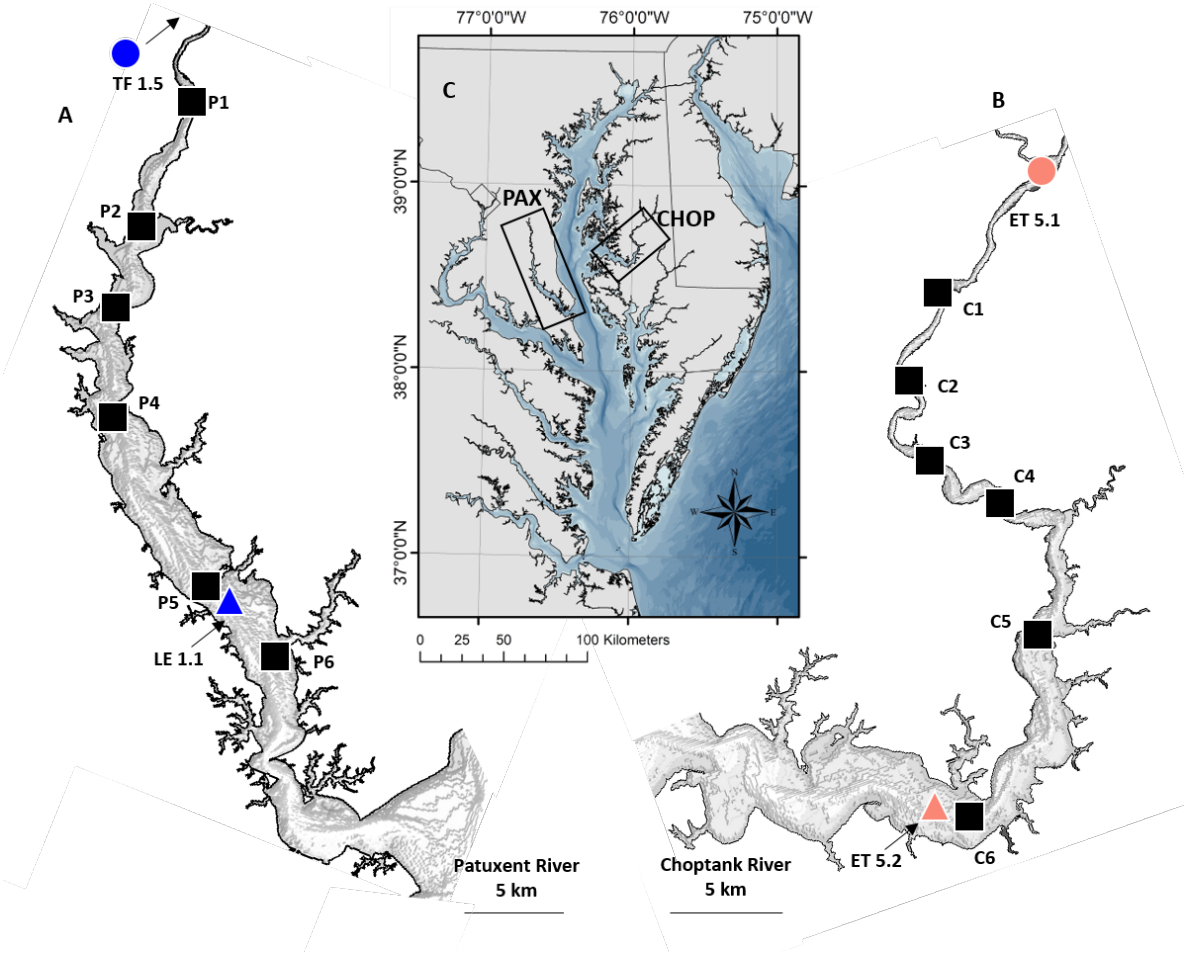

Figure 2. Average monthly dissolved oxygen concentration (DO), salinity, water temperature, and chlorophyll-a concentration (Chl-a), measured at Chesapeake Bay Program Long-term Water Quality Monitoring Program stations in the tidal fresh-oligohaline (Oligo) and mesohaline (Meso) regions of each river (shaded regions represent sampling intervals). Box plots of monthly pairwise differences between rivers from January 2018 to December 2019 shown at right (data above or below the dashed line interpreted as higher values in the CHOP or PAX, respectively).

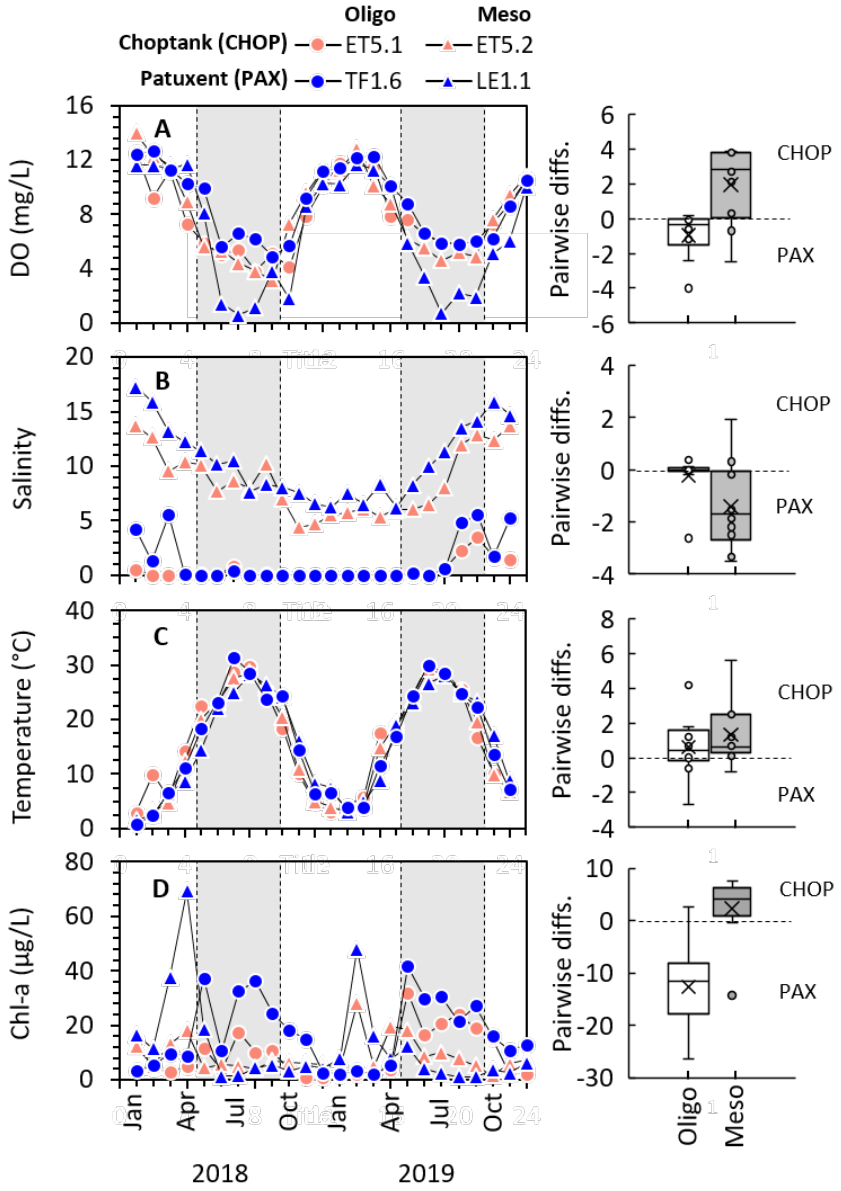

Figure 3. Haplotype network for *Neomysis americana* across samples from the Chesapeake Bay and St. Lawrence Estuary. Depicted is a randomized minimum spanning tree (RMST) network for *N. americana* CO1 haplotypes in Chesapeake Bay, USA (Patuxent River, Pax; Choptank River, Chop) and the St. Lawrence Estuary, Canada (Marine Transition Zone, STL-MTZ; Estuarine Site, STL-ES). Each circle/pie represents a unique haplotype and size of the pie chart corresponds to the frequency or number of haplotypes represented (see legend). Colors of the pie charts correspond to the sampling location and mutational steps between haplotypes are shown as dots.

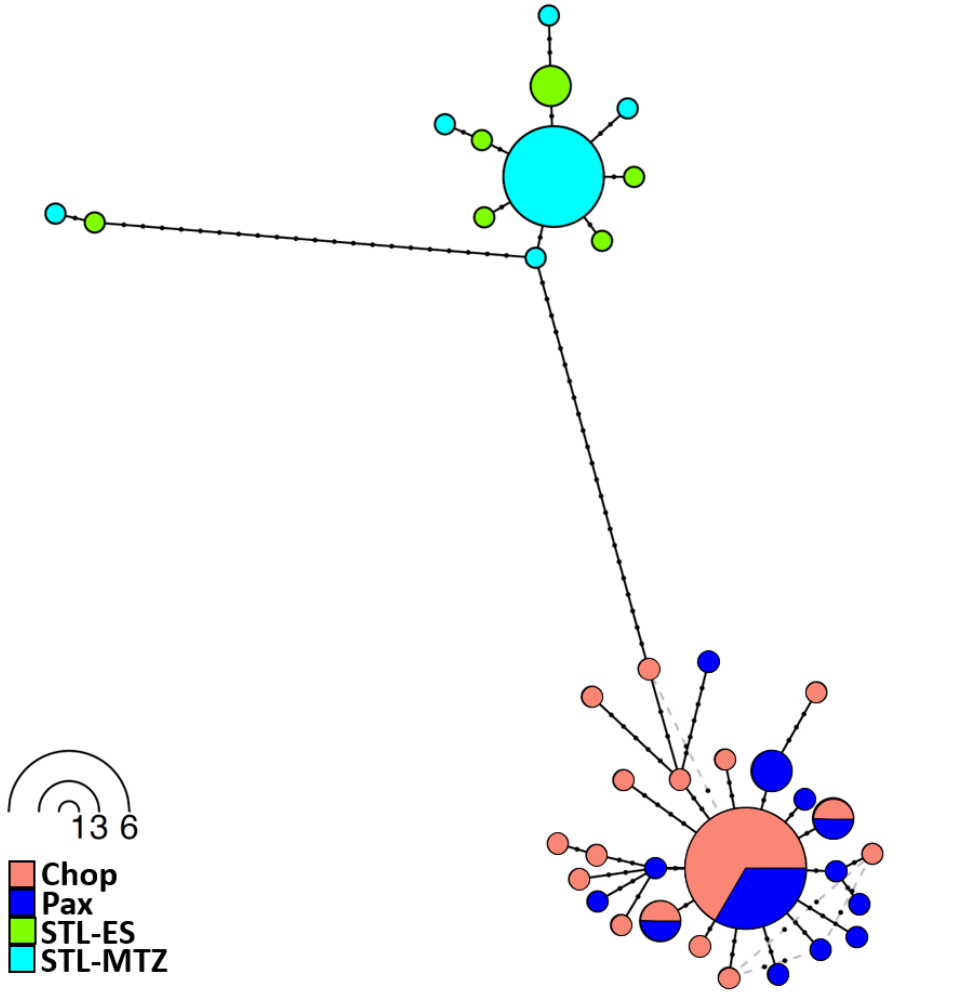

Figure 4. Neighbor joining tree of *Neomysis americana* haplotypes with distances calculated via the p-distance method. Sample names in bold are from the current study ($N = 51$), italics are from Cortial et al. (2019; $N = 18$), and the outgroup is the congener *Neomysis integer*. Bootstrap $n = 999$ replicates (only branches with > 85% confidence shown). Tree is drawn to scale, branch length units = evolutionary distances used to infer phylogenetic tree (p-distance). Sample prefixes: St. Lawrence Estuary, Canada (MTZ, ES [Marine Transition Zone, Estuary Site) and Chesapeake Bay, USA (C, P [Choptank River, Patuxent River]). Lineages A, B, and C from Cortial et al. (2019) are shown for the three main groupings or clades within the tree.

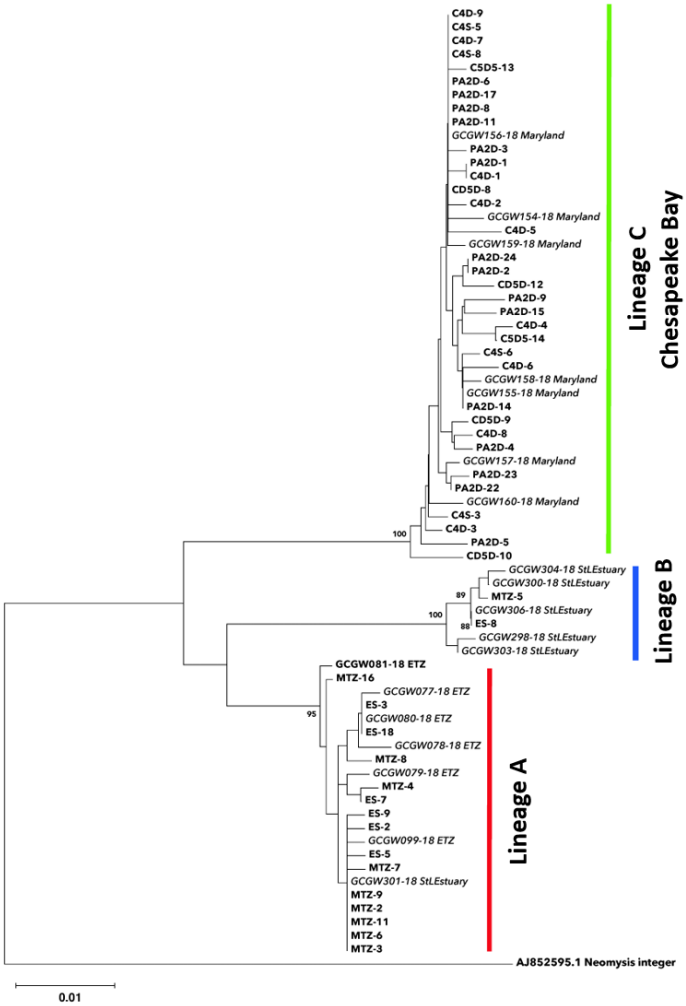

Figure 5. Size-structure of *Neomysis americana* (assigned to 1-mm size bins) included in growth rate (A, $N = 1{,}225$) and clutch size calculations (B, $N = 307$). Observed clutch size (C_t) of gravid *N. americana* plotted against female body length from early summer (Early: May, June) and late summer (Late: August, September) with iteratively reweighted least-squares fitted regression lines (dashed lines) from generalized linear models for Patuxent (C, $N = 145$) and Choptank (D, $N = 162$) rivers. Inset photo in panel B shows gravid female *N. americana* collected from the Tred Avon River, Choptank River complex, Chesapeake Bay, Maryland.

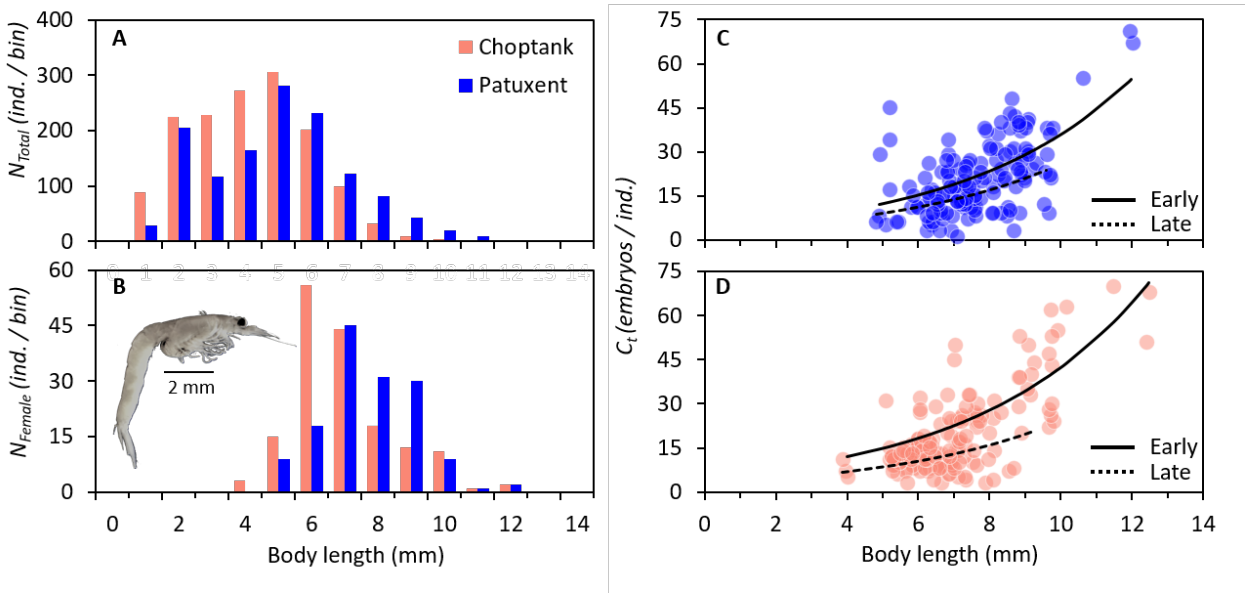

Figure 6. Generalized linear model predictions of clutch size (C_t) and size-specific clutch size (C_{ss}) at three body lengths (L_f) = 5, 8.5, and 12 mm for *Neomysis americana* sampled from the Choptank (Chop) and Patuxent (Pax) rivers in early summer (Early: May, June) and late summer (Late: August, September). No 12-mm estimates provided for late summer predictions as no gravid females with L_f > 10 mm were collected during that season; error bars are +/- 1 SE.

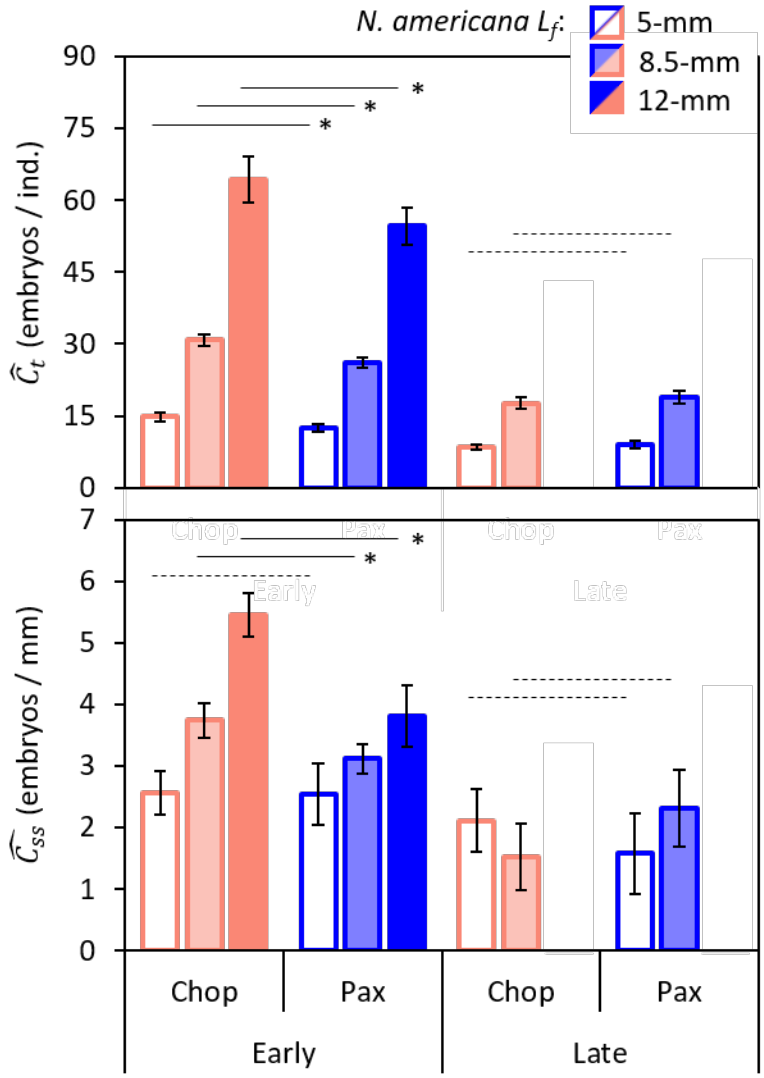

Figure 7. Ratio of embryo length (E_l, mm) to clutch size (C_t) plotted against female body length (L_f, mm) for Stage I (N = 108), II (N = 100), and III (N = 36) embryos of *Neomysis americana* from 2018 in the Choptank and Patuxent rivers, Chesapeake Bay, MD (A, lines are least-squares fitted regressions for each embryo stage). Least-squares means (+/- SE) estimate of residuals around E_l:C_t vs L_f fitted curves for each tributary (B; residuals are different at $p < 0.0001$).

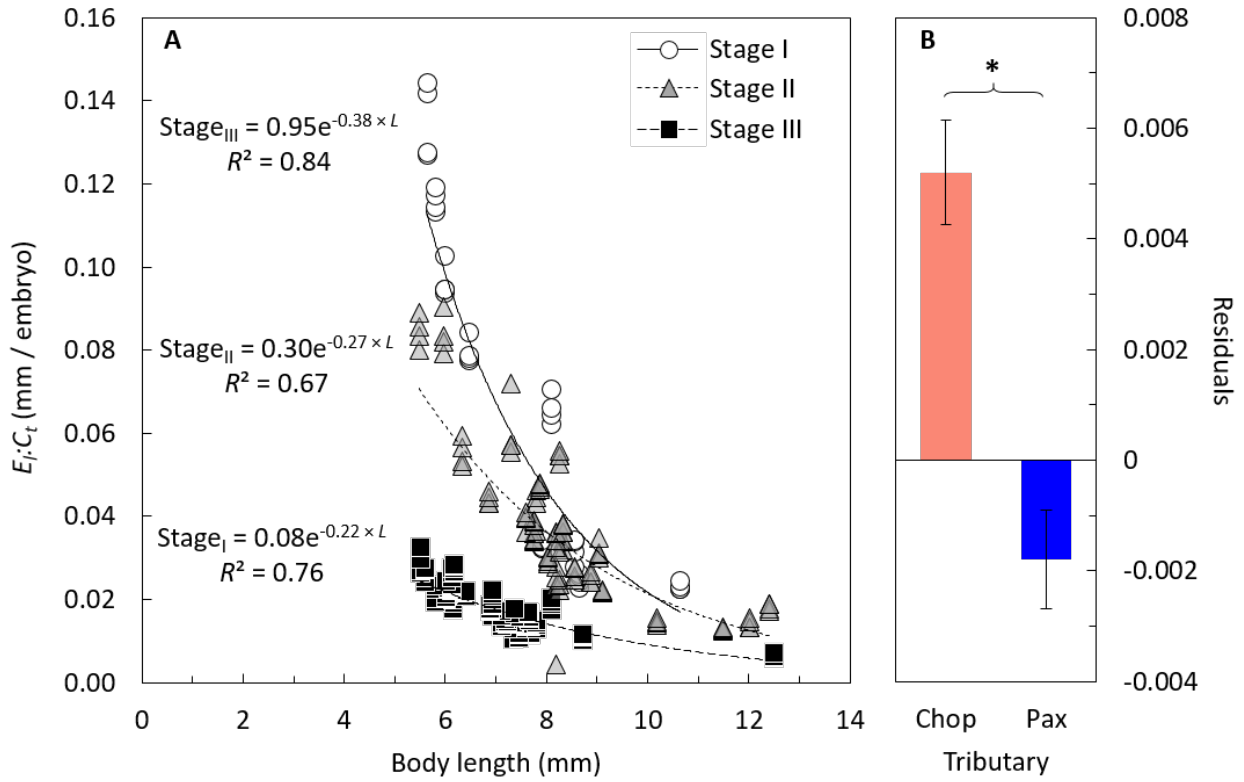
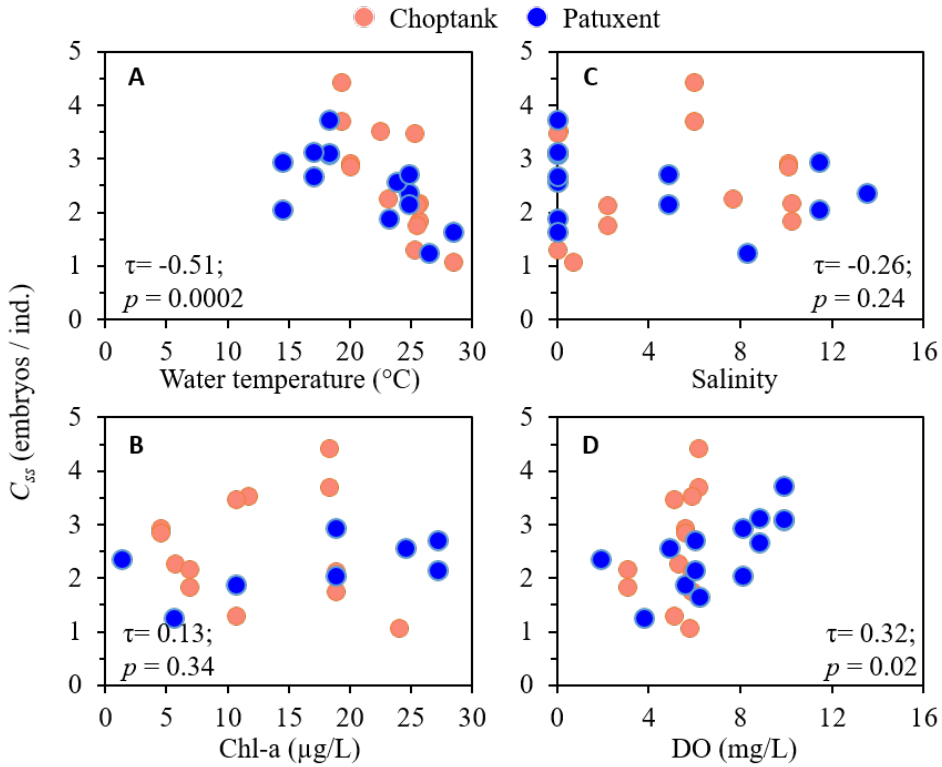
Figure 8. Average monthly size-specific clutch size (C_{ss}) plotted against average monthly water temperature, chlorophyll-a concentration (Chl-a), salinity, and dissolved oxygen concentration (DO) measured at Chesapeake Bay Program Long-term Water Quality Monitoring Program stations proximal to mysid sampling stations in each river (see Figure 1). Kendall's tau correlation coefficient and significance (τ, p-value [$\alpha = 0.05$]) between C_{ss} and each water quality variable shown.